2010 NDIA GROUND VEHICLE SYSTEMS ENGINEERING AND TECHNOLOGY SYMPOSIUM
MODELING & SIMULATION, TESTING AND VALIDATION (MSTV) MINI-SYMPOSIUM
AUGUST 17-19 DEARBORN, MICHIGAN

SIMULATION OF VARIOUS ON-BOARD VEHICLE POWER GENERATION ARCHITECTURES FOR STATIONARY APPLICATIONS

Matthew Young
Angela Card
Stephen Phillips
G. Marshall Molen
Jim Gafford
Mike Mazzola
Center for Advanced Vehicular System
Mississippi State University
Starkville, MS

ABSTRACT

As more electrical-based systems are developed for battlefield use, the mobile and stationary power requirements of military vehicles continue to increase. Current power requirements of the light and medium duty class military vehicles' 28 VDC system are exceeding what is achievable from a single alternator system that is belt-driven. In-service, belted alternator systems, such as the C803 Niehoff alternator (28 VDC, 520 A), are capable of providing up to 14.5 kW of electrical power at the maximum speed of the alternator. However, during stationary applications, these systems are only capable of producing 7.7 kW at an engine idle speed of 700 RPM. For these systems to be able to comply with the 10 kW plus power requirement, additional vehicle control is needed to elevate engine speed to an appropriate level to ensure the required power output may be achieved. For power levels above 15 kW, single-machine, belt-driven solutions become impracticable. This paper evaluates various power generation architectures that could meet the stationary requirements without the need for engine speed control on otherwise conventional (non-hybrid-electric) vehicles. Three architectures are considered in this study; all three include the original-equipment belt-driven alternator, making legacy or vehicles currently in production the most relevant platforms. The cases studied are as follows: dual alternators that are belt-driven, a combination of a belt-driven alternator and a transmission power-take-off (PTO) driven alternator, and a combination of a belt-driven alternator and a PTO-driven Permanent Magnet Brushless DC (PMDC) machine. The simulations account for power transfer efficiency for each of the proposed architectures and derive the total power required from the power sources to meet the desired load profile. The proposed architectures are compared based on the total energy required by the engine for running the 28 VDC power systems.

INTRODUCTION

Current military on-board power systems are required to provide total generated power levels from 10 kW up to 30 kW [1]. With the C.E. Niehoff 28 V 520 A alternators on military vehicles today, these systems are capable of providing up to 14.5 kW at the rated speed of the alternator. However, during stationary applications when the engine is at idle speed, the installed alternator is only capable of producing a maximum of 7.7 kW [2]. In order to reach a 10 kW stationary power requirement, additional engine speed control must be deployed to elevate the vehicles engine speed to ensure safe operation of the alternator.

The need for a speed control system to meet the current power requirements introduces excessive audible noise, increased thermal signature, and fuel usage. Some of these consequences may cause additional safety risks to the soldier. Therefore, speed control systems are not considered in this paper. Beyond the speed control concern, original equipment alternators are becoming insufficient, by themselves, to meet increased warfighter requirements for 28 VDC power. Many short-terms solutions to this problem are clearly not capable of meeting objective requirements for exportable AC power, so alternative options should be considered. The global emergence of hybrid vehicles has opened an opportunity for the deployment of high power-

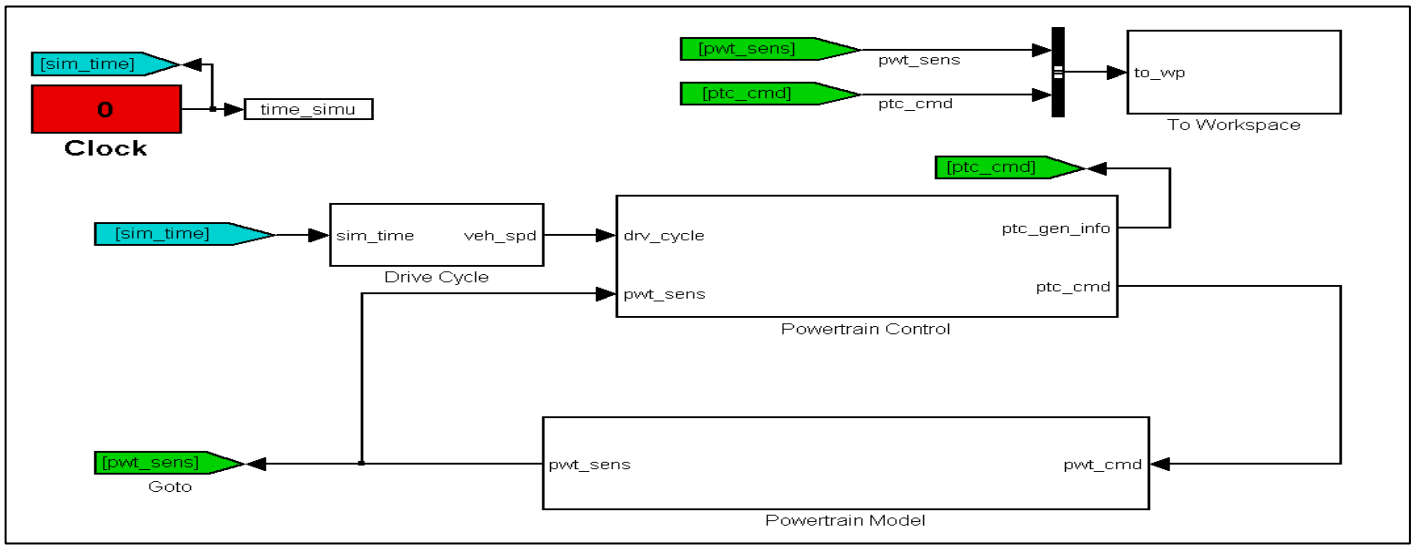

Figure 1: Top-level layout of simulation environment for evaluation of various power generation architectures

density electric machines for use in on-board power generation systems. These machines could allow higher power levels at low speeds. For instance, current electric machines used in traction drive applications have the capability to provide upwards of 30 kW of generation power at relatively low speeds with an appropriate alternator to engine ratio[3-4]. In addition to the high power density of these systems, they are typically more efficient when compared to high-current alternators currently in use.

This paper presents the development and results of a power generation system simulation used for the evaluation of three types of power generation architectures: a dual alternator system where both alternators are belt-driven, a system consisting of a primary belt-driven alternator with a supplemental power take-off (PTO)-driven alternator, and a belt-driven alternator with a PTO- driven permanent magnet DC (PMDC) machine.

POWER GENERATION SYSTEM SIMULATION

A top-level layout of the designed simulation environment is shown in Figure 1 using Simulink. The simulation environment was implemented by taking a forward-facing approach. Forward-facing refers to the direction of the calculations within the model. In this environment, a commanded vehicle speed or torque request initiates the simulation and component outputs are consequently calculated through the drivetrain to the wheels [5]. A forward-facing simulation approach provides a tradeoff between required simulation time, transient modeling, and control system development. This approach is consistent with popular drivetrain modeling software PSAT and ADVISOR [6-7].

For the simulation model shown in Figure 1, the powertrain controller receives vehicle speed information from the 'Drive Cycle' subsystem. For the purpose of this paper, the requested vehicle speed is held at zero for the duration of the stationary simulation. Electrical load information, in terms of electrical power required, is gathered from feedback sent by the 'Powertrain Model'. The required load is used by the 'Powertrain Control' subsystem to generate a torque request for all electrical generation components in the system. Each of the analyzed power system architectures shares some fundamental operating constraints:

- Maintain 28 V battery state-of-charge at 80%.
- No component allowed to operate outside maximum capacity.
- Primary alternator required to supply first 50 A of current to ensure proper charging of 28 V battery using the internal voltage regulator.
- Primary alternator required to supply at least 2 A charging current to 28 V battery.

Along with forcing all components to conform to the system constraints, the 'Powertrain Control' subsystem is also responsible for implementing the selected current sharing strategy. Each architecture studied in this paper has a unique strategy for sharing the electrical load. The load sharing strategies are designed to distribute electrical load based on the selected pulley or gear ratios and maximum output power capability for each of the components in the system. In addition to sharing the electrical load between the components, each strategy can be customized so a desired amount of additional electrical load can be requested from a given system component. This additional electrical load could represent power exported to a DC or AC load.

POWER GENERATION ARCHITECTURES

Three power system architectures were evaluated using the above mentioned simulation environment. Each architecture incorporates an original-equipment belt-driven alternator similar to that found on many Army ground vehicles. The C.E. Niehoff 28 V, 520 A alternator is assumed to be the primary vehicle power source supplied as original equipment. Each architecture differs by the method assumed to supplement the original equipment while meeting the load profile. The C.E. Niehoff alternators are capable of providing up to 14.7 kW of electrical power at the rated speed of the machine. However, at engine idle speeds with the selected pulley ratio, the maximum power output of the alternator is approximately 7 kW [2]. Plots of alternator efficiency and electrical power output are shown in Figure 2 as a function of alternator speed.

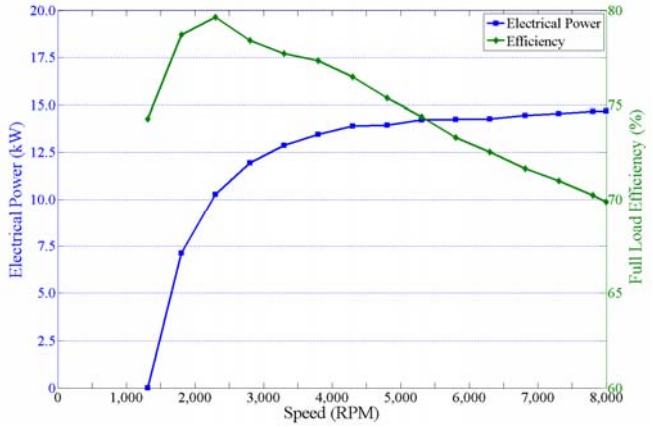

Figure 2: Alternator electrical power output (blue line) and efficiency (green line) versus speed

All belt-driven alternator systems used a pulley ratio of 3:1 from alternator input shaft to engine crankshaft. Each belt-driven system is assessed a power transfer loss of 5%. This 5% transfer loss assumes that the drive belts of the alternators are newly installed and tensioned properly [8]. The following sections discuss the 'Powertrain Model' and 'Powertrain Control' for each of the simulated power system architectures.

Architecture 1: Dual Alternators that are Belt-Driven

This architecture is comprised of dual alternators that are belt-driven. It utilizes most closely the prevailing technology deployed in current military vehicles. This architecture employs two identical alternators connected to the engine via a crankshaft pulley and belt. A diagram of Architecture 1 is shown in Figure 3.

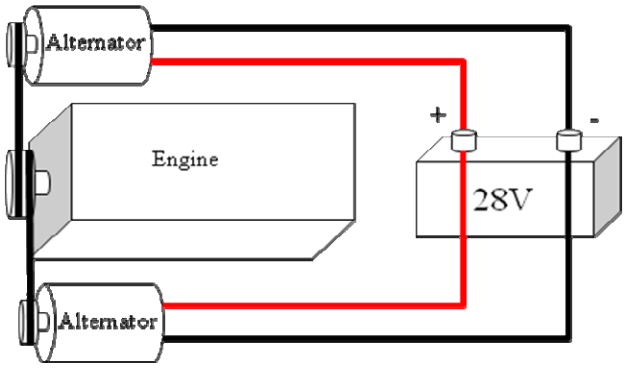

Figure 3: Configuration of Architecture 1

The 'Powertrain Control' subsystem for Architecture 1 functions as a simple current sharing system. Each alternator is commanded to contribute 50% of the requested load up to its maximum power capability. This approximates a system of two nearly identical alternators placed in parallel, each utilizing a standard voltage regulator with a slightly positive internal resistance characteristic.

Architecture 2: Primary belt-driven alternator with a supplemental power take-off (PTO)-driven alternator

This architecture assumes that a second alternator of the same performance as the primary (OEM) alternator is added but interfaced to the engine through the transmission's power-take-off (PTO) port. The PTO-drive portion of this architecture utilizes a total gear ratio of 2.54:1 from alternator to engine crankshaft. This gear ratio was selected to ensure the alternator would not over speed at the engine maximum speed. Additionally, the gear ratio was selected so a gearbox could be designed with the least number of gears for higher efficiency and be constructed as small as possible. The overall power transfer efficiency for the PTO-mounted gearbox was estimated to be 97%. Figure 4 provides a system diagram of Architecture 2.

The 'Powertrain Control' subsystem for Architecture 2 uses a slightly different control algorithm as compared to the previous architecture. The difference in drive ratios between belt-driven and PTO-driven alternators produces a 15% speed difference which produces a 25% difference in available output power. For this reason, in the simulation the belt-driven alternator generates 25% more electrical power than the PTO-driven alternator.

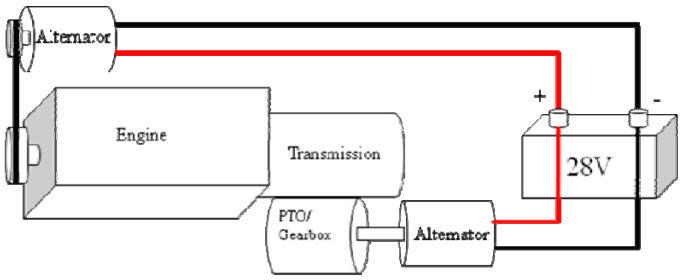

Figure 4: Configuration of Architecture 2

Architecture 3: Belt-Driven Alternator and PTO-Driven PMDC

The final architecture selected for evaluation is similar to the previous architecture but assumes a major component change. The PTO driven alternator is replaced with a power dense high-efficiency PMDC system. This system includes the PMDC machine and necessary motor control/inverter. The high voltage DC output is coupled with a high-current DC/DC converter which is used to supplement the 28 V vehicle bus with electrical current. The architecture diagram is shown in Figure 5.

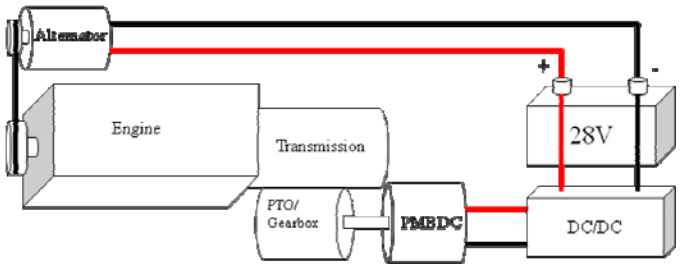

Figure 5: Configuration of Architecture 3

Using the same approach as the previous architecture, the PMDC machine is connected to the vehicle driveline via a PTO adapter and gear box. The overall gear ratio for the PTO-drive system is set to 2.15:1 from input shaft of the PMDC to engine crankshaft. With the selected gear ratio, the PMDC machine will operate at an input speed of 1750 RPM at engine idle and will provide a maximum of 35 kW intermittent and 20 kW continuous electrical power. Figure 6 shows the maximum electrical power output with machine efficiency at various speeds. The transfer efficiency of the PTO-drive system and electrical conversion efficiency of the DC/DC converter was estimated to be 98%.

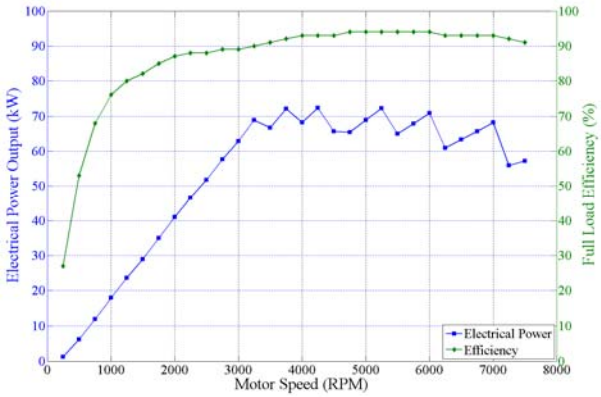

Figure 6: PMDC machine rated electrical power output (blue line) and efficiency (green line) versus input speed.

The 'Powertrain Control' subsystem for this architecture was developed to utilize the higher efficiency of the PMDC machine for loads greater than a desired threshold. The threshold was used to ensure proper battery charging using the alternator's internal regulator. The simulated power sharing control algorithm was constrained as described in the Power Generation System Simulation section. Additionally, the output power of the DC/DC converter was limited to a level that would allow the entire system (primary alternator and PMDC machine) to meet a near-term application goal of supplying 600 A at 28 VDC. An appropriately rated commercially available DC/DC converter suitable for installation in a medium-sized Army ground vehicle is the Air Cooled 7 kW unit made by Absopulse. The 'Powertrain Control' subsystem is programmed to provide the first 50 A of load current from the primary alternator. Incremental load increases above 50 A are supplied by the PMDC through the DC/DC converter until the load reaches 270 A total. Loads in excess of 270 A is provided by the primary alternator and the PMDC with the DC/DC converter maintaining a constant 250 A output. The rated current of the alternator at a particular engine speed limits the total load current that can be supplied above 270 A.

SIMULATION RESULTS

The three chosen architectures were evaluated using a dynamic load profile taken from a radar system. The load profile shown in Figure 7 provides electrical power requests both above and below the rated power output of any single component of the chosen architectures. Using the load profile shown above, each architecture simulation computes the power required from the engine to meet the desired electrical load. This required power is integrated throughout the simulation time to determine the total energy consumption. Assuming a constant engine efficiency of 25%

and converting the energy consumption required by the selected architectures from BTUs to gallons of JP-8 fuel, the total fuel consumption of each of the architectures can be compared. Figure 8 presents the cumulative fuel used during the simulation, assuming an engine efficiency of 25%, for each of the architectures tested.

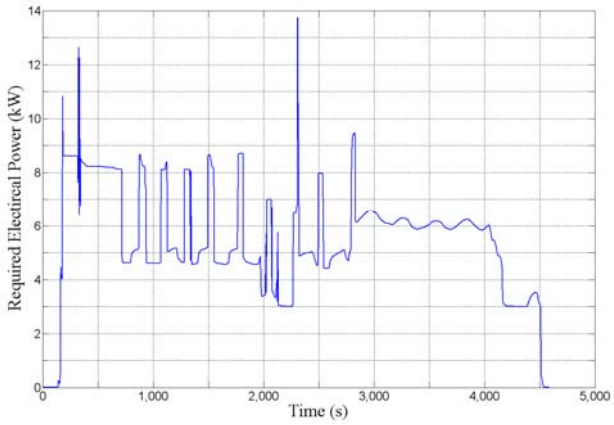

Figure 7: Load Profile used for simulation of all three power system architectures

In addition to computing fuel consumption, the simulation calculates overall system efficiencies. Figure 8 shows the calculated overall system efficiency for each architecture during the simulation. Architecture 3 provides the highest efficiency output of any of the three architectures. This is due to the higher operating efficiency of the PMDC system. However, the operating efficiency of the PMDC based system is still below 60% because it is operating under relatively light load in relation to the rated capacity of the PMDC at its idle operating speed. In order to simulate the possible capability of the PMDC based system, an additional simulation was conducted which added 10 kW of additional load to the PMDC side of the system. This additional power might be drawn from an external AC or DC load. Note, only Architecture 3 is augmented with the assumed external load because it alone has the available spare capacity.

Figure 10 shows the calculated system efficiency and fuel used during the simulation using both the standard load profile and the additional 10 kW PMDC electrical load. It can be seen that the overall system efficiency shown in Figure 10 is over 10% higher than the system efficiency of the same architecture as shown in Figure 9. This increase in system efficiency is due the additional load place on the PMDC machine forcing it into a high efficiency region.

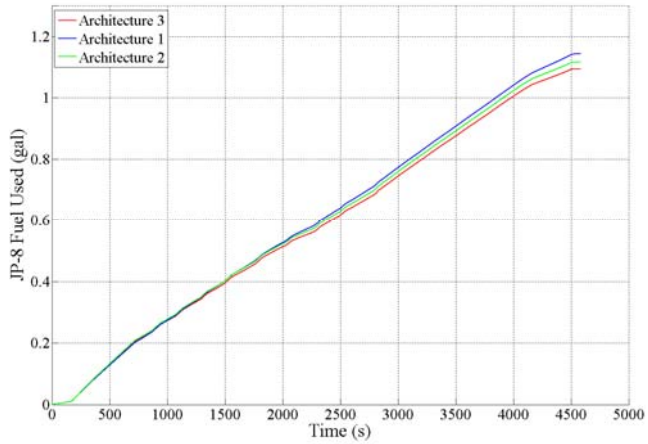

Figure 8: JP-8 fuel consumption for each architecture assuming 25% engine efficiency

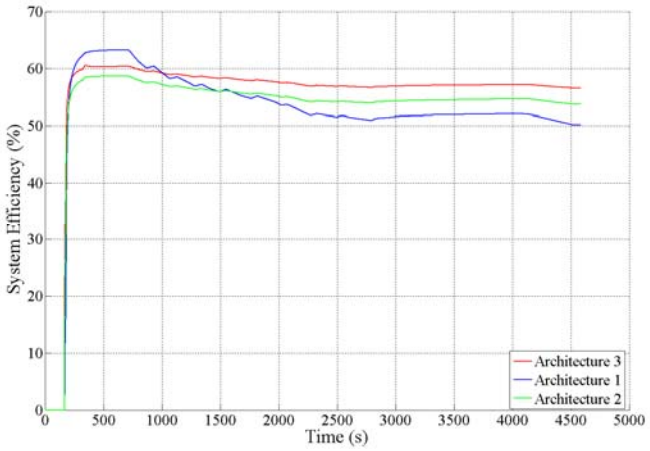

Figure 9: Overall architecture system efficiencies

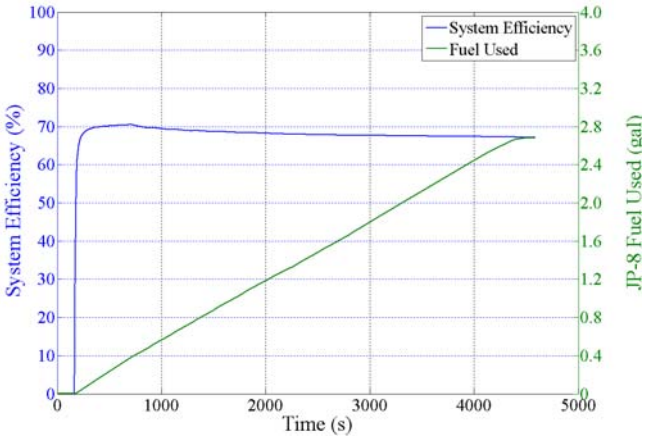

Figure 10: Belt-driven alternator and PTO-driven PMDC system efficiency and fuel consumption with additional 10 kW AC load applied to PMDC system

CONCEPT EVALUATION OF ARCHITECTURE 3 (A BELT-DRIVEN ALTERNATOR AND PTO-DRIVEN PMDC)

Based on the simulation results presented above, an empirical evaluation on a vehicle with an original equipment belt-driven alternator retrofitted with a PTO-driven PMDC power system was conducted. The architecture was developed for evaluation on a Mine Resistant Ambush Protected (MRAP) vehicle. The components used for the architecture evaluation include:

- 28V 520 A belt-driven C.E. Niehoff alternator with 3:1 pulley ratio
- UQM PowerPhase75 PMDC machine connected to an Allison transmission's PTO output using a cogged belt-drive system with a 1.8:1 drive ratio

Once the power system components were integrated into the vehicle's drivetrain, an initial load evaluation was conducted. The load contribution of the belt-driven alternator and PTO-driven PMDC was conducted as presented above. The system evaluation was conducted using load steps of 50 A to an intermediate load plateau of 250 A. When the system reached the intermediate load level, the load was removed to evaluate the systems reaction to load shedding. After load shedding was successfully demonstrated, the intermediate load was reapplied and load steps of 50 A were added until the load reached 400 A, at which point a second load transient evaluation was successfully conducted. Load steps were continued until a final design load of 600 A was reached. The system was allowed to operate at 16.8 kW for an extended period to evaluate individual component operating stability (electrically, mechanically, and thermally) at elevated loads. At the design load, the measured current output of the alternator system was 370 A while the PMDC system was supplying 240 A. Stable static and dynamic electrical load sharing was observed. Figure 11 shows the PMDC system mounted into the test vehicle.

Figure 11: PMDC power system mounted in test vehicle

CONCLUSION

It has been shown that the three power system architectures examined through simulation are all viable options for increasing the stationary load capability of large format military vehicles. Table 1 provides a summary of the architectures evaluated through simulation in terms of total fuel used in gallons and overall system efficiency. Of the three architectures examined, the architecture using the PTO-driven PMDC machine is the most fuel efficient while also providing spare power generating capacity for future requirements. This architecture was examined further in an empirical evaluation. The hardware implementation studied the feasibility of integrating power system components into a legacy vehicle drivetrain and the performance of the load sharing methodology. Superb performance was observed.

Table 1: Summary of architecture simulations

Architecture	Fuel Consumption	System Efficiency
1 (Dual alternators)	1.14 gals	50.2 %
2 (Belt-driven and PTO-driven alternators)	1.12 gals	53.7 %
3 (Belt-driven alternator and PTO-driven PMDC)	1.09 gals	56.6 %
3(Belt-driven alternator and PTO-driven PMDC) with additional 10 kW AC load	2.69 gals	67.1 %

REFERENCES

[1] G. Mulcahy and J. Santini, "Next Generation Military Vehicle Power Conversion Modules", TDI Power, Online: http://www.tdipower.com/PDF/white_paper/WP_militar militaryvehic.pdf, 2008.

[2] "500-A Neihoff Alternator Datasheet", C.E. Niehoff, Online: http://www.ceniehoff.com

[3] M. Marcel, J. Schultz, and G. Grider, "DRS-TEM On-Board Vehicle Power System", NDIA Ground-Automotive Power and Energy Workshop, 2008.

[4] "PowerPhase® 75", UQM Technologies, Online: http://www.uqm.com/pdfs/PP75%20Spec%20Sheet%20 2.21.10.pdf

[5] D. Gao, C. Mi, and A. Emadi, "Modeling and Simulation of Electric and Hybrid Vehicles", *Proceedings of the IEEE*, vol. 95, no. 4, pp. 729-745, April 2007.

[6] A. Rousseau, "PSAT Overview" Online: http://www.transportation.anl.gov/pdfs/HV/412.pdf.

[7] T. Markel *et. al*., "ADVISOR: a systems analysis tool for advanced vehicle modeling", Journal of Power Sources, Volume 110, Issue 2, 22 August 2002, Pages 255-266.

[8] "Replace V-Belts with Cogged or Synchronous Belt Drives", The Office of Industrial Technologies, Online: http://www.nrel.gov/docs/fy00osti/27833.pdf